

# Visually evoked local field potential changes in the caudate nucleus are remarkably more frequent in awake, behaving cats than in anaesthetized animals

DIÁNA NYUJTÓ<sup>1</sup>, ÁDÁM KISS<sup>1</sup>, BALÁZS BODOSI<sup>1</sup>,  
GABRIELLA EÖRDEGH<sup>2</sup>, KÁLMÁN TÓT<sup>1</sup>, ANDRÁS KELEMEN<sup>3</sup> and  
ATTILA NAGY<sup>1\*</sup> 

<sup>1</sup> Department of Physiology, Faculty of Medicine, University of Szeged, Szeged, Hungary

<sup>2</sup> Faculty of Health Sciences and Social Studies, University of Szeged, Szeged, Hungary

<sup>3</sup> Department of Applied Informatics, University of Szeged, Szeged, Hungary

Received: May 22, 2023 • Revised manuscript received: October 19, 2023 • Accepted: November 19, 2023

Published online: January 31, 2024

© 2023 The Author(s)



## ABSTRACT

Previous results show that halothane gas anaesthesia has a suppressive effect on the visually evoked single-cell activities in the feline caudate nucleus (CN). In this study, we asked whether the low-frequency neuronal signals, the local field potentials (LFP) are also suppressed in the CN of anaesthetized animals.

To answer this question, we compared the LFPs recorded from the CN of two halothane-anaesthetized (1.0%), paralyzed, and two awake, behaving cats during static and dynamic visual stimulation. The behaving animals were trained to perform a visual fixation task.

Our results denoted a lower proportion of significant power changes to visual stimulation in the CN of the anesthetized cats in each frequency range (from delta to beta) of the LFPs, except gamma. These differences in power changes were more obvious in static visual stimulation, but still, remarkable differences were found in dynamic stimulation, too. The largest differences were found in the alpha and beta frequency bands for static stimulation. Concerning dynamic stimulation, the differences were the biggest in the theta, alpha and beta bands.

\* Corresponding author. H-6720 Szeged, Dóm tér 10. Tel.: +36 62 545869; fax: +3662545842. E-mail: nagy.attila.1@med.u-szeged.hu

Similar to the single-cell activities, remarkable differences were found between the visually evoked LFP changes in the CN of the anaesthetized, paralyzed and awake, behaving cats. The halothane gas anaesthesia and the immobilization suppressed the significant LFP power alterations in the CN to both static and dynamic stimulation. These results suggest the priority of the application of behaving animals even in the analysis of the visually evoked low-frequency electric signals, the LFPs recorded from the CN.

## KEYWORDS

visual, local field potential, power spectrum analysis, halothane anaesthetized cat, behaving cat

## INTRODUCTION

Beside the prominent role of the caudate nucleus (CN) in motor processes, it is also involved in sensory information processing through cortical and subcortical loops in the mammalian brain [1, 2]. The primary source of the visual inputs to the basal ganglia is the ascending tectofugal visual system, which sends the information from the superior colliculus through the posterior thalamus to the CN. The CN also receives visual cortical inputs from the anterior ectosylvian cortex [3]. These inputs are responsible for the specific visual properties of the CN. Previous studies denoted that the CN neurons are sensitive to static and dynamic visual stimuli, too [4–13]. The particular spatial and temporal visual properties of the CN neurons, i.e., preferences for low spatial and high temporal frequencies and narrow spatiotemporal spectral tuning [9, 14] suggest the contribution of these neurons to motion and novelty detection. Thus, the CN seems to belong to those brain structures that have the capacity to sample and evaluate a wide variety of changes in the visual environment.

The control of eye movements is obligatory in visual electrophysiological experiments because of various reasons. First of all, the spatial position of the visual stimulus has to overlap with the receptive field of the investigated neuron. Additionally, several visually active brain structures possess visuomotor activity, such as saccadic responses [15, 16]. Therefore, the researchers must eliminate the effect of eye movements on neuronal activities. Acute, anaesthetized, paralyzed, and awake, behaving animals are often used in visual electrophysiological research. Both models have their own advantages and disadvantages. The work in acute animals seems to be easier because there is no long behavioural training to restrict eye movement prior to the electrophysiological recordings [13, 17]. On the other hand, this increases the number of animals sacrificed, and the anaesthetics can also influence the activity of the brain. The deep brain sensorimotor structures, i.e., the cerebellum and the basal ganglia, are extremely sensitive to anaesthesia [18, 19]. Single-cell activity analysis revealed significant differences between the neuronal activities recorded from the feline CN in anaesthetized and behaving cats. The anaesthesia and the immobilization significantly suppressed the neuronal activity and the visual responsiveness of the CN. Furthermore, it was almost impossible to analyse phasically active neurons, the dominant neuronal population of the CN, due to the low neuronal activities. [20]. These results suggest the necessity of the behaving animals if the activity of the single CN cell is the focus of the research. The training and preparation of cats is often a challenging process that may last up to 9 months [17, 20]. Beside single cell activities, the low-frequency signals (local field potentials = LFPs) can also carry information from the visual environment. The visually



evoked LFP changes can give information about the sum of the cortical and subcortical visual inputs in the CN. The question raises whether the LFP activities and the visually evoked LFP changes are suppressed similarly in the anaesthetized animals as the single-cell activities. To address these questions, we compared the LFPs recorded from the CN in halothane anaesthetized, paralyzed, artificially ventilated and awake, behaving cats. An earlier study denoted that the median of visual onset response latencies was 100 ms in the CN (the range was 20–200 ms, [11]. Additionally, the CN is involved in novelty detection and the detection of changes in the visual environment [2, 9]. We have focused on the alterations in different frequency bands (theta, alpha, beta, and gamma) of the LFPs in the first 320 ms time after the appearance of the static visual stimulus, and in the first 320 ms after the starting of the movement of the dynamic visual stimulus.

## MATERIALS AND METHODS

We recorded from the CN of two halothane anaesthetized, paralyzed, and two awake, behaving adult, domestic cats that weighed between 2.5 and 5 kg. The acute recordings lasted for 3 days. The recording sessions of the behaving cats lasted 30 min to 1 hour per day, four to five times a week.

All procedures were performed to minimize the number and the discomfort of the animals, and the experimental protocol was accepted by the Government Office based on the suggestion of the Ethical Committee for Animal Research of Albert Szent-Györgyi Medical and Pharmaceutical Centre at the University of Szeged (No.: XIV./518/2018 and XIV/1818/2021) and was conducted in full accordance with the Directive 2010/63/EU of the European Parliament and the Council on the Protection of Animals Used for Scientific Purposes and the guidelines of the Committee.

### Surgical procedure of the anaesthetized animals

The animals were initially anaesthetized with ketamine hydrochloride (Calypsol (Gedeon Richter LTD), 30 mg kg<sup>-1</sup> i.m.). A subcutaneous injection of 0.2 ml 0.1% atropine sulphate was administered preoperatively to reduce salivation and bronchial secretion. All wound edges and pressure points were treated regularly with a local anesthetic (1% procaine hydrochloride). The trachea and the femoral vein were cannulated, and then the animals were placed in a stereotaxic frame. The cats were artificially ventilated with 1.2–1.6% halothane during surgery, which was reduced to 0.8–1.0% during the recording sessions to minimize the effects of anaesthesia. The depth of the anaesthesia was monitored continuously with the end-tidal anaesthetic concentration and heart rate. The minimal alveolar anaesthetic concentration (MAC) values calculated from the end-tidal halothane concentration were kept in a recommended range [21]. The end-tidal halothane concentration, MAC values and the peak expired CO<sub>2</sub> concentrations were monitored with a capnometer (CapnomacUltima, Datex-Ohmeda, ICN). The O<sub>2</sub> saturation of the capillary blood was monitored by pulse oximetry. The peak expired CO<sub>2</sub> concentration was kept within the range of 3.8–4.2% by adjustment of the respiratory rate or volume. The animals were immobilized with an initial 2 ml intravenous bolus of gallamine triethiodide (Flaxedil, 20 mg kg<sup>-1</sup>, Sigma, St. Louis, MO, USA). During the whole experiment, a mixture containing gallamine triethiodide (8 mg kg<sup>-1</sup> h<sup>-1</sup>), glucose (10 mg kg<sup>-1</sup> h<sup>-1</sup>) and



dextran ( $50 \text{ mg kg}^{-1} \text{ h}^{-1}$ ) in Ringer lactate solution was infused continuously at a rate of  $4 \text{ mL h}^{-1}$ . The body temperature of the cats was maintained at  $37^\circ\text{C}$  by an electric heating blanket. Craniotomy was performed with a dental drill to allow a vertical approach to the target structures. The dura mater was removed, and the skull hole was covered with a 4% solution of  $37^\circ\text{C}$  agar dissolved in Ringer's solution. The eye contralateral to the subcortical recording site was treated locally with atropine sulphate (one or two drops, 0.1%) and phenylephrine hydrochloride (one or two drops, 10%) to dilate the pupils, block accommodation and retract the nictitating membranes, and was equipped with a +2 diopter contact lens. During the recordings, the ipsilateral eye was covered.

### Visual paradigm and recording in anaesthetized animals

The recording sessions took place in a dark, quiet room where the background luminance was  $2 \text{ cd m}^{-2}$ . Vertical penetrations made within the Horsley-Clarke coordinates anterior 14 mm and lateral 4–5 mm, at a stereotaxic depth of 10–15.3 mm. The extracellular electrophysiological recordings were carried out with a 64-channel 2 shank (32 channel/shank, diameter:  $300 \mu\text{m}/\text{shank}$ ) platinum-iridium linear probe (Neuronelektród Ltd., Hungary). The vertical distance between each channel was  $50 \mu\text{m}$ . The reference electrode was a  $125 \mu\text{m}$  tungsten electrode which was inserted in the white matter in the position of anterior 7 and lateral 8 according to the Horsley-Clarke coordinates. The electrical signals were amplified and digitalized with Intan rhd 2132 chips and Hinstra Dendas data acquisition system (Hinstra Instruments Ltd., Hungary). Amplified neuronal activities were recorded at a 20 kHz sampling rate and stored for offline analysis. The stimulus presentation was controlled by a custom-made software and was presented on an 18-inch CRT monitor (refresh rate: 100 Hz) 57 cm in front of the animal. A single trial (one repetition of the whole stimulation protocol) consisted of 3 epochs (phases): first a blank, black screen was presented to obtain background activity without visual stimulation for 2000 ms; then a random dot pattern appeared on the screen for 1,500 ms as a stationary stimulus; that was followed by the dynamic stimulus, where the same white dots started to move randomly either toward the periphery (center-out flow field) or toward the center (center-in flow field) of the screen. The dynamic stimulus also lasted 1,500 ms. The size of each dot was  $0.1^\circ$  in diameter in both the static and the dynamic stimulus. The speed of dot movement increased from 0 to  $7^\circ/\text{s}$  toward the periphery. One recording session lasted 15 min, where 50 trials were presented from for each of the center in and center out conditions in a pseudo-random order. Between the recordings, the electrode position was changed ( $200 \mu\text{m}$  downward), and a 30-min break was kept before the next recording.

### Surgical procedure in case of awake, behaving animals

The preparation before the surgery was carried out the same way as with the anaesthetized animals. First, the cats were initially anaesthetized with ketamine hydrochloride (Calypsol (Gedeon Richter<sup>®</sup>),  $30 \text{ mg kg}^{-1}$  i.m), then a subcutaneous injection of  $0.2 \text{ ml}$  0.1% atropine sulphate was administered. In addition, a preventive dose of antibiotic (1,000 mg ceftriaxon, i.m., Rocephin 500 mg (Roche<sup>®</sup>)) was given preoperatively. The surgical preparation started with the cannulation of the femoral vein, then continued with the implantation of a scleral search coil (Cooner wire, Owensmouth, CA, USA) into one eye to monitor the eye movements of the cats during the recordings [17, 22–27]. After the intubation of the trachea, the cats were placed in a



stereotaxic frame. All pressure points and wounds were treated with local anesthetic (1% procaine hydrochloride). During the surgery, the anesthesia was maintained with 1.5% halothane in a 2:1 mixture of  $\text{N}_2\text{O}$  and oxygen. The depth of the anesthesia was monitored by continuously checking the end-tidal halothane concentration, MAC values, the peak expired  $\text{CO}_2$  concentrations and the  $\text{O}_2$  saturation. Firstly, a stainless steel head-holder was installed on the skull to fixate the head during the recordings. After this, the craniotomy was performed with a dental drill; the dura mater was preserved, and the skull hole was covered with a 4% solution of 38 °C agar dissolved in Ringer's solution. Then a reclosable plastic recording chamber (20 mm in diameter) was cemented on the skull to avoid any contamination and to protect the microdrive system and the extracellular electrodes. Following this, eight wire electrodes covered by a guiding tube were implanted above the CN according to the Horsley-Clarke coordinates anterior 12–14 mm, lateral 4–6.5 mm. Recordings were performed at the stereotaxic depths between 10 and 16 mm. The electrodes were implanted in the brain with the help of an adjustable microdrive system [28, 29].

On the first five postoperative days, ceftriaxone antibiotic was administered intramuscularly (Rocephine, 50 mg  $\text{kg}^{-1}$ ). Nalbuphin (0.25 mg  $\text{kg}^{-1}$ ) and non-steroidal anti-inflammatory drugs were administered until the seventh postoperative day.

### Behavioural training of awake, behaving cats

The detailed description of the training process and the recordings can be found in our previous studies [13, 17, 20]. The cats were suspended in the experimental stand by a canvas harness. The cats were trained to perform the behavioural fixation paradigm while their heads were fixed to the stereotaxic frame. The stereotaxic frame with the animal was placed within an electromagnetic field, which is generated by metal coils installed into the wall of the experimental stand. During the fixation training, the fixation time was gradually increased from 100 to 2500 ms. Square fixation windows were used. The size of the initial fixation window was  $\pm 10^\circ$  for both cats. During the training period, it was reduced to  $\pm 2.5^\circ$  in  $\pm 2.5^\circ$  steps. The animals were trained to hold their eyes in the center of the monitor during recordings of neuronal activities to different kinds of visual stimulation. The behavioral training lasted 9–12 months approximately 1–2 hours per day, four to five times a week. The training phases and later the recordings took place in a dark, quiet laboratory room.

### Visual paradigm and recordings in case of awake, behaving cats

The electrophysiological extracellular recordings were carried out with perylene isolated platinum-iridium wire-electrodes with a diameter of 25  $\mu\text{m}$  for the first cat; and formvar insulated nickel-chrome wire-electrodes with a diameter of 50  $\mu\text{m}$  for the second cat. Each recording electrode contained 8 wires and one wire contained one recording channel. The reference electrode was positioned in the white matter in anterior 3 and lateral 8 according to the Horsley-Clarke coordinates. The recording of the eye movements, stimulus presentation, reward delivery, and data collection were controlled by a custom-made LabView software via a 16-channel National Instruments data acquisition card. The sampling rate was 10 kHz. Eye movements were monitored and recorded with a search coil system (DNI Instruments, Newark, DE, USA). A standard 17-inch CRT monitor (refresh rate: 100 Hz) was placed in front of the animal at a viewing distance of 57 cm for the visual stimulation. The fixation point and



the visual stimuli were generated by a custom-made script written in Matlab and using the Psychophysics Toolbox® [30]. A fixation point was projected on the center of the monitor to help maintain the fixation on the middle of the monitor during the relevant stimulus phases. The size of the fixation point was  $0.8^\circ$  in diameter, the fixation window was  $5^\circ$  in diameter ( $5^\circ \times 5^\circ$  square). In the case of the behaving, awake animals, a trial (one repetition of the whole stimulation protocol) consisted of 5 epochs (phases). First, a green fixation point was presented in the center of the monitor. The cats had to direct their gaze to the fixation point and keep fixating for 500 ms. The visual stimulation task started immediately after the successful fixation phase. It means that the cat held his eye in the above described  $\pm 2.5^\circ$  fixation window. This was similar to the stimulation used in the anaesthetized experiments: a static random dot pattern appeared first, which was followed by a dynamic center-in or center-out flow field stimulation in random order. The duration of both the static and the dynamic stimuli was 1,000 ms. If the cats managed to fixate throughout all the stimulation phases of a single trial, they received a food reward, and it was considered a correct trial. If the cats broke fixation during any of the stimulation phases, the trial was aborted immediately, it was not accepted, and no reward was given. Between two trials, there was a random 5,000–10,000 ms long intertrial interval (reward was given at the beginning of this time range), where no stimuli appeared, only a black screen. This phase was long enough so that the cat could eat the reward without muscle activity interfering with the recordings of the next trial. One recording session lasted 30–45 min. The number of successful trials, where the animal could hold the fixation during the whole stimulation protocol, were analyzed. These varied between 80 and 200 in each recording.

## Data analysis

For the data analysis and the statistical analysis, Matlab R2021a software (The Mathworks, Natic, MA, USA) was used. During the analysis, the power of the delta (1–3 Hz), theta (4–7 Hz), alpha (8–13 Hz), beta (14–30 Hz), and gamma (31–70 Hz) bands were calculated.

The first step was the visual inspection of the recorded raw data (Fig. 1). Channels with high amplitude noise and/or bad signal-noise ratio were excluded from further analysis. After the subtraction of these channels, the downsampling of the remaining channels was performed for further mathematical analysis. It was done by applying a low pass filter and decimation to 500 Hz for the raw data using the Matlab *decimate* function. After the downsampling of the original dataset, Fourier analysis was performed. The power spectrum was then video-filtered (smoothed) by a ten-bin rectangle window. A whitening compensation was used to visualize higher frequency bands more equally, however, the calculations were made from the original raw data. After the whitening, a median filter (Matlab *medfilt1*) was also used with the default parameters. During the visualization of the Fourier spectra, the bins near 50 Hz were cut off.

## Filtering and power calculation

The raw data of each channel was decimated to 500 Hz by the Matlab *decimate* function. The decimation filter was an finite impulse response filter (FIR) one, and its length was chosen to 20 ms, not to alias brain events through each other.

For each band, a digital superheterodyne test receiver was implemented. The center frequency of every band was shifted to 0 Hz by multiplying the signal with a complex rotating vector. After this step, a Chebyshev infinite impulse response filter (IIR) filter was used, and the



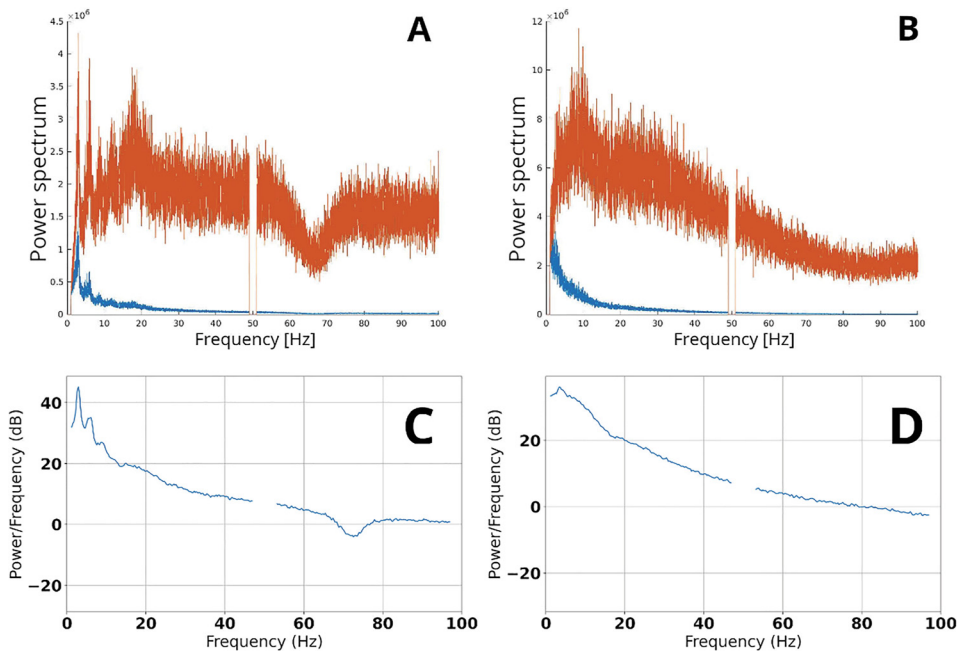


Fig. 1. Spectral image of the LFP recordings

Part A shows the Fourier spectrum of a recorded signal (Cecilia589\_ch4) from a behaving cat. Part B denotes the Fourier spectrum of a recorded signal (Igor067\_ch11) from an anaesthetized cat. The blue colour shows the raw Fourier spectrum and the orange colour denotes the whitened one. Part C and Part D denote the spectral power of the same recorded signals calculated with the Welch function

signal was decimated to a lower sampling frequency. The filtering and decimating steps were repeated in order to reach the desired width of the band, and fulfil the stability criteria of the filters (Fig. 2). The final decimation was done for 25 Hz. For the theta signal (the lowest interesting frequency band in this study), the resulting stable filters require a 25 Hz sampling frequency. Calculating the power of signals hence shows  $t = 1/f = 40$  ms time resolution. The higher frequency band was also summated and decimated with the same time resolution and sampling frequency. Having the 25 Hz complex signal for each band, the absolute value of these signals represents the power of the signal for each 40 ms wide sample.

## Statistical analysis

The powers of a randomly selected 320 ms period (the average of eight 40 ms wide bins (samples described above) from the background activity and 320 ms periods (the average of eight 40 ms wide samples described above) immediately after the appearance of the stationary stimulus and the start of the dynamic stimulus were calculated in each trial and each frequency band, both in the behaving and the anaesthetized LFP recordings. The powers of these 320 ms periods in each frequency band from all trials were non-normally distributed (Shapiro-Wilk  $P < 0.05$ ). Thus, they were compared with the Friedman ANOVA test with Bonferroni correction both in the



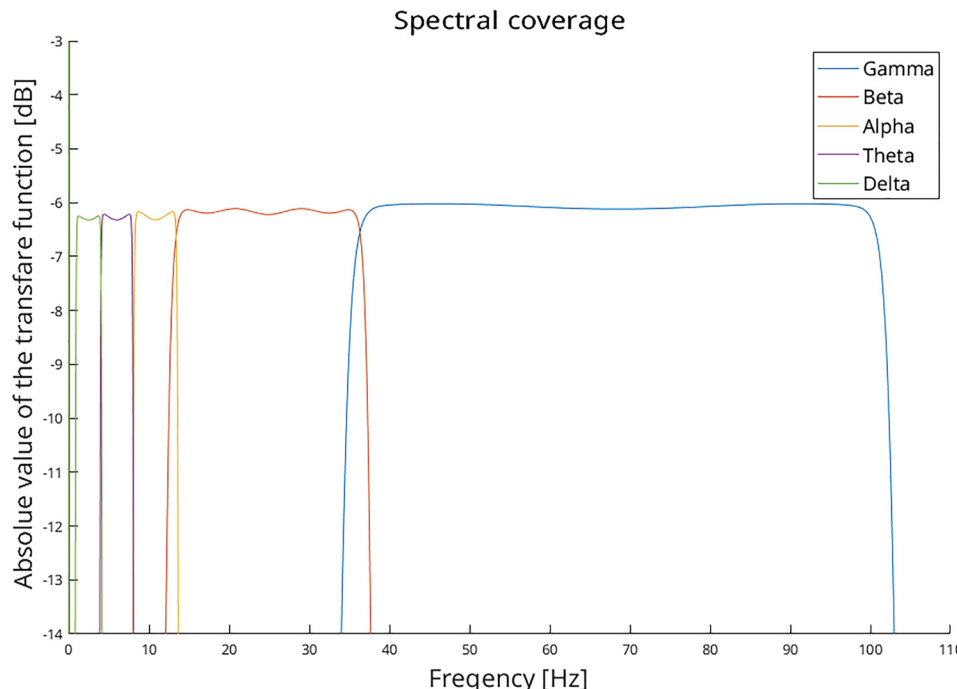


Fig. 2. Spectral coverage of the applied band pass filters

The characteristics of the filters in each frequency band can be seen with different colors (green-delta, purple-theta, yellow-alpha, orange-beta, blue-gamma) section. Note the overlap between the frequency-based neighbouring filters and their sharp filtering properties

behaving and anaesthetized LFP recordings. If this test denoted a significant difference ( $P < 0.05$ ) in one LFP recording, it would indicate that at least one of the three conditions (background activity, response to static or dynamic stimulation) differs from the others. In this case, the Wilcoxon matched pair test was used for a pairwise comparison as a post hoc analysis to check which part of the stimulated activity (static, dynamic, or both) differs significantly from the background activity the different frequency bands. The significant differences from the background activity were considered in the present study as dynamic and static visual responses in the CN.

## RESULTS

Altogether 226 local field potential (LFP) recordings from awake, behaving cats and 960 LFP recordings from anaesthetized cats were involved in the data analysis. Each LFP recording (which contained at least 80 trials) was analysed separately. The LFPs were analysed in five different frequency bands (delta (1–3 Hz), theta (4–7 Hz), alpha (8–13 Hz), beta (14–30 Hz), and gamma (31–70 Hz)).



The summary of the detailed descriptive statistics can be seen in [Table 1](#). Comparing the response activity during visual stimuli to the background activity, Wilcoxon matched pair test revealed that 90% ( $N = 207$ ) of all registered LFPs from awake, and only 63% ( $N = 609$ ) from the anaesthetized cats showed significant responses at least in one visual condition (static, dynamic) and one frequency band. [Figure 3](#) denotes examples of the visually evoked power changes in the awake, behaving, and [Fig. 4](#) in anaesthetized animals.

*Table 1.* Descriptive statistics of visually evoked LFPs during visual stimuli from awake, behaving, and anaesthetized animals

	Awake ( $N = 226$ )		Anesthetized ( $N = 960$ )	
	N	%	N	%
Delta	80	35	168	17
Theta	98	43	178	19
Alpha	121	56	181	19
Beta	144	64	210	22
Gamma	53	23	220	23
All	204	90	609	63

In awake animals the percentage of LFPs that showed significant changes to visual stimulation in delta, theta, alpha and beta frequency band was higher than in the anesthetized animals.

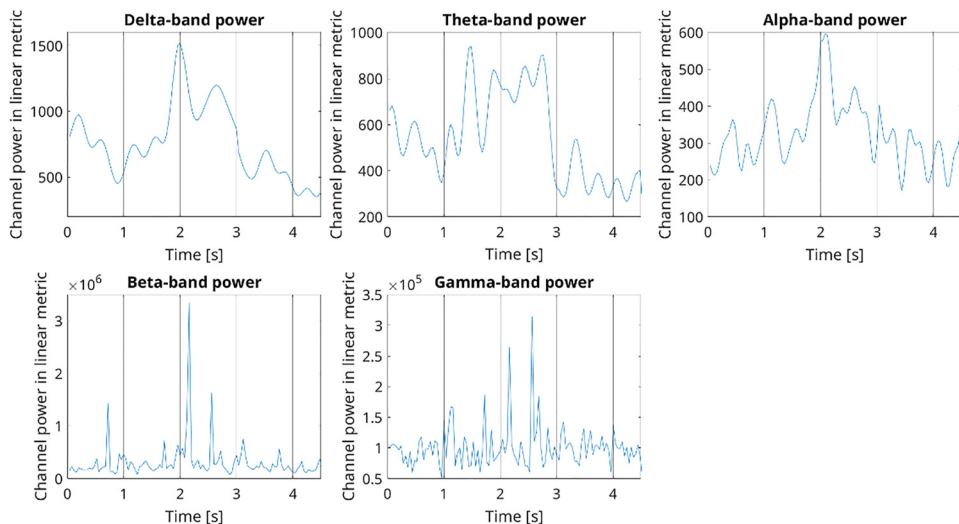


*Fig. 3.* Visually evoked changes of the local field potentials in awake animal

Cumulated power of the wave bands (from delta to gamma) after applying the given spectral filter (see [Fig. 2](#)) for each frequency band. The blue curve represents the mean activity for all trials. The vertical lines denote the borders between the different epochs of the visual paradigm (from left to right): background activity, fixation activity, response to static visual stimulus, response to dynamic visual stimulus and reward. The abscissa denotes the time relationship of the signals. The ordinate denotes the channel power in linear metrics



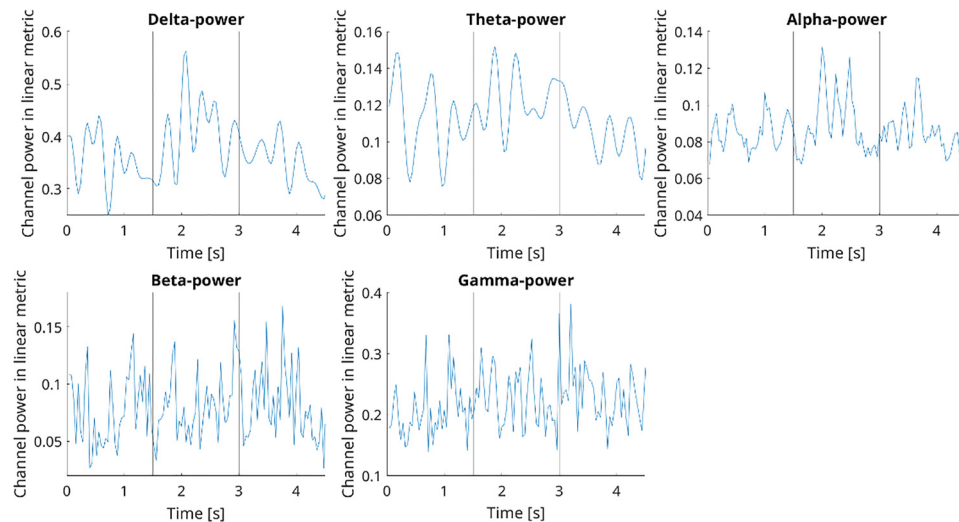


*Fig. 4.* Visually evoked changes of the local field potentials in halothane anaesthetized cat Cumulated power of the wave bands (from delta to gamma) after applying the given spectral filter for each frequency band. The blue curve represents the mean activity for all trials. The vertical lines denote the borders between the different epochs of the visual paradigm (from left to right): background activity, response to static visual stimulus and response to dynamic visual stimulus. The abscissa denotes the time relationship of the signals. The ordinate denotes the channel power in linear metrics

The percentage of LFPs that showed significant changes to static and/or dynamic stimulation in theta, alpha and beta frequency bands was higher in awake, behaving cats. In the theta band, the percentage was 43% ( $N = 98$ ) in awake and only 19% ( $N = 178$ ) in anaesthetized cats. In the alpha band, the percentage was 56% ( $N = 121$ ) in awake and 19% ( $N = 181$ ) in anaesthetized cats. In the beta frequency band, the percentage of the significant LFPs was 64% ( $N = 114$ ) in awake and 22% ( $N = 210$ ) in anaesthetized cats. In the gamma frequency band, the percentage of the significant LFP changes was 23% in both ( $N = 34$ ) the awake and the anaesthetized cats (Table 1).

### Responses to static visual stimulation

The proportion of LFPs that showed significant response during static visual stimulation was much higher in awake, behaving cats (83%,  $N = 122$ ) than in anaesthetized cats (63%,  $N = 177$ ). A higher percentage of visually evoked LFP changes can be observed in almost each frequency range in the behaving animals. The only exception is the theta band where the same percentages were found (Wilcoxon match paired test, see descriptive statistical data in Table 2). These differences are the most obvious in the alpha and the beta frequency bands. In the case of the alpha band, the percentage was 49% ( $N = 110$ ) in awake and only 24% ( $N = 228$ ) in anaesthetized cats. In the case of the beta band the percentage of the significant LFP changes was 49% ( $N = 110$ ) in behaving cats, and it was only 23% ( $N = 221$ ) in anaesthetized cats.



Table 2. Descriptive statistics of response activity during static and dynamic visual stimuli

	Static				Dynamic			
	Awake (N = 226)		Anesthetized (N = 960)		Awake (N = 226)		Anesthetized (N = 960)	
	N	%	N	%	N	%	N	%
Delta	68	30	178	19	61	27	218	23
Theta	58	26	282	29	89	39	183	19
Alpha	110	49	228	24	76	34	147	15
Beta	110	49	221	23	69	31	203	21
Gamma	72	32	225	23	46	20	215	22
All	187	83	602	63	172	76	611	64

Higher percentage of visually evoked LFP changes during static stimulation can be observed in the delta, alpha, beta, gamma frequency range in the behaving animals. This tendency can be observed in the theta, alpha, beta frequency bands during dynamic visual stimulation.

### Responses to dynamic visual stimulation

In comparison to the effect of the static stimulation (83%, N = 187) a bit lower amount of the analysed LFPs showed significant changes to dynamic stimulation (76%, N = 172) in behaving cats. However, the percentage of the responsive LFPs to static and dynamic stimulation were similar in the anaesthetized animals, 63% (N = 602) and 64% (N = 611), respectively.

Similarly, to the static visual stimulation, the proportion of LFPs that showed significant responses during dynamic visual stimulation was higher in awake, behaving cats (76%, N = 172) than in anaesthetized ones (64%, N = 611, Wilcoxon match paired test, see descriptive statistical data in Table 2). These differences are the most notable in the theta, alpha and the beta frequency bands. In the case of the theta band, the percentage was 39% (N = 89) in awake, and only 19% (N = 183) in anaesthetized cats. In the alpha band the percentage was 34% (N = 76) in the behaving animals and 15% in the anaesthetized cats. The percentage of the significant LFP changes was 31% (N = 69) in behaving, and it was lower 21% (N = 37) in anaesthetized cats in the beta frequency band.

## DISCUSSION

To our knowledge, this is the first descriptive study that compares the low-frequency neuronal activities (local field potentials, LFPs) recorded from the CN during visual stimulation in anaesthetized, paralyzed, and awake, behaving cats. In line with the findings of our previous study on the single cell activities [20], the present results clearly demonstrated that the applied halothane anesthesia indeed suppresses the visually evoked LFP changes at a remarkable level. Thus, lower proportion of significant power changes was detected to visual stimulation in the anaesthetized animals in each frequency range (from delta to gamma) of the LFPs.

In visual electrophysiological experiments, both anaesthetized, paralyzed, and awake, behaving models are commonly used. Both have their advantages and disadvantages. The control of eye movements in visual electrophysiology is critical. The spatial position of the visual



stimulus must overlap with the receptive field of the investigated neuron, and oculomotor activity can also be found in some extrastriate visual structures [15, 16]. If one would like to eliminate these disturbing factors, there are two possibilities. In anaesthetized and paralyzed animal models, eye movements are inhibited through muscle relaxants. However, the applied anesthetics and muscle relaxants can influence the activity of the central nervous system. It is also assumed that this effect is not the same as in the cortex or the deeper brain structures [31]. The basal ganglia are strongly sensitive to different kinds of anesthesia [18, 19]. In the case of the single-cell activities in the CN, the anesthesia influences the timing of the action potential and the discharge rates significantly [20]. Beside these high-frequency signals, the LFPs could also be influenced. Based on our previous experiences that the halothane influences the neuronal activities less in the CN than other gas anesthetics (i.e., isoflurane), although we cannot exclude the effect of the anesthesia from the results in anaesthetized animals. The big advantage of the application of this anaesthetized animal is the quick application of it without any training of the animals. The second solution for the elimination of the effect of eye movements on neuronal activities is the application of eye movement controlled fixating behaving animals. The disadvantage of the experiments with behaving animals is the long-lasting behavioral and fixation training, which could last for 9–12 months before the start of the electrophysiological recordings. However, there is no disturbing effect of anesthetics in this case.

The question raises whether the benefit of experiments performed in the CN of awake, behaving animals is in balance with the hardness of the preparation of the animals for visual electrophysiological recordings. The results of the visual information processing in the CN revealed that both the background activities and the neuronal responses to static and dynamic visual stimulation were strongly reduced in the anaesthetized animals. The most drastic differences can be seen in the biggest neuronal population in the medium spiny neurons of the caudate body [20]. Concerning the significant changes in LFP in response to visual stimulation, the differences between the two models are also obvious. The vast majority (90%) of the LFPs recorded in behaving cats showed significant responses at least in one visual condition (static, dynamic) and one frequency band. On the other hand, it was a smaller proportion of the LFPs (61%) in anaesthetized cats. These differences in power changes were the stronger concerning static visual stimulation (83% vs 63%). Less, but still obvious differences were found to dynamic stimulation, too (76% vs 64%). The higher proportion of the evoked LFP responses were detectable in both static and dynamic stimulation in each investigated frequency band from the lower delta to the highest gamma band. However, the biggest differences were concerning static stimulation in the alpha and the beta frequency bands and concerning dynamic stimulation to the theta, the alpha and the beta bands.

Similar to human EEG results, the increased theta activity could arise from the coordinated reactivation of information represented in visual areas [32–36]. The elevated cortical alpha activity is also connected to visual and audio-visual processing [37–39]. Another function that has been attributed to alpha activity is a mechanism of sensory suppression, thus functionally gating information in the task-irrelevant brain areas [40, 41]. It is also assumed that the normal beta activity is a necessary cortical outcome of the normal action of the basal ganglia in visual information processing [42]. Since the analysis addressed the first 320 ms time window of both static and dynamic stimulation, novelty detection and the connected sensory gating could be the task that shows these differences between the anaesthetized, paralyzed, and awake, behaving animals [2, 9].



Beyond the lack of halothane anesthesia and immobilization, our behaving model differed from anaesthetized models also in a third way: both eyes of the animal were open during stimulation (in anaesthetized cats, recordings are made only from one eye, while the other eye is covered, [43]). This monocular-binocular difference could influence the magnitude of visual responses, but such strong difference, as seen in this study, is not likely to stem from this factor only [44-46]. It is noteworthy to mention that the anaesthetized cats were cycloplegic, and the awake ones had normal pupils and lenses, but in the case of anaesthetized cats the visus was corrected with appropriate lenses. As the background luminance was the same for the two models and the same CRT monitor was used, these do not explain the observed difference either. An important shortcoming of the study is that the recordings from behaving and anaesthetized cats were performed with different recording systems with different background noise levels. Thus, the direct comparison of the magnitude of the visual responses was not possible in this study. Therefore, we could only concentrate on whether the changes were significant or not and we could give the presented a descriptive statistic about the percentage of these visually-evoked changes. Another limitation is that electrodes with different geometries were applied in the behaving (wire electrodes) and anaesthetized (linear probe) experiments. It is known that the geometry of the electrodes could influence the magnitude of the recorded LFPs [47]. But if we compare the baseline power spectrum density of one channel with the power spectrum density during visual stimulation of the same channel, it will not influence the number of significant changes and the differences between the two models. The different electrodes, 8-channel wire electrodes in the behaving experiments, and 64-channel linear probes in the anaesthetized experiments, explain the higher number of recorded LFPs from the anaesthetized animals.

To summarize our findings, we demonstrated similarly to the single cell activities [20], marked differences between the visually evoked LFP changes in the CN of the anaesthetized, paralyzed, and awake, behaving cats. The halothane gas anesthesia and the immobilization significantly suppressed the significant LFP power alterations to both static and dynamic stimulation. Although the work with behaving cats in visual electrophysiology is much more difficult, we argue that the benefits outweigh the costs, and we suggest the application of the behaving animal model even in the analysis of the low-frequency electric signals, the LFPs.

**Funding:** This work was supported by a grant from SZTE ÁOK-KKA Grant No. 2019/270-62-2 and SZTE SZAOK-KKA-SZGYA Grant No: 2023/5S479.

**Author contributions:** DN, GE, and AN designed the study; DN, GE, KT, NA and BB performed the assessment and documented the findings; ÁK, AK and NA analysed the data; DN, ÁK, AK, BB and NA organized the study and wrote the manuscript.

**Competing interest:** The author(s) declare no competing interests (both financial and non-financial).

## ACKNOWLEDGEMENTS

The authors thank to Siposné Gabriella Dósai-Molnár and László Rácz for the technical assistance and to Robert Averkin for the microdrives and the wire electrodes.



## REFERENCES

1. McHaffie JG, Stanford TR, Stein BE, Coizet V, Redgrave P. Subcortical loops through the basal ganglia. *Trends Neurosci* 2005; 28(8): 401–7. <https://doi.org/10.1016/j.tins.2005.06.006>.
2. Benedek G, Keri S, Nagy A, Braunitzer G, Norita M. A multimodal pathway including the basal ganglia in the feline brain. *Physiol Int* 2019; 106(2): 95–113. <https://doi.org/10.1556/2060.106.2019.09>.
3. Rokszin A, Markus Z, Braunitzer G, Berenyi A, Benedek G, Nagy A. Visual pathways serving motion detection in the mammalian brain. *Sensors (Basel)* 2010; 10(4): 3218–42. <https://doi.org/10.3390/s100403218>.
4. Strecker RE, Jacobs BL. Substantia nigra dopaminergic unit activity in behaving cats: effect of arousal on spontaneous discharge and sensory evoked activity. *Brain Res* 1985; 361(1–2): 339–50. [https://doi.org/10.1016/0006-8993\(85\)91304-6](https://doi.org/10.1016/0006-8993(85)91304-6).
5. Rolls ET, Thorpe SJ, Maddison SP. Responses of striatal neurons in the behaving monkey. 1. Head of the caudate nucleus. *Behav Brain Res* 1983; 7(2): 179–210. [https://doi.org/10.1016/0166-4328\(83\)90191-2](https://doi.org/10.1016/0166-4328(83)90191-2).
6. Hikosaka O, Sakamoto M, Usui S. Functional properties of monkey caudate neurons. II. Visual and auditory responses. *J Neurophysiol* 1989; 61(4): 799–813. <https://doi.org/10.1152/jn.1989.61.4.799>.
7. Chudler EH, Sugiyama K, Dong WK. Multisensory convergence and integration in the neostriatum and globus pallidus of the rat. *Brain Res* 1995; 674(1): 33–45. [https://doi.org/10.1016/0006-8993\(94\)01427-j](https://doi.org/10.1016/0006-8993(94)01427-j).
8. Nagy A, Eordeghe G, Benedek G. Extents of visual, auditory and bimodal receptive fields of single neurons in the feline visual associative cortex. *Acta Physiol Hung* 2003; 90(4): 305–12. <https://doi.org/10.1556/APhysiol.90.2003.4.3>.
9. Nagy A, Paroczy Z, Markus Z, Berenyi A, Wypych M, Waleszczyk WJ, et al. Drifting grating stimulation reveals particular activation properties of visual neurons in the caudate nucleus. *Eur J Neurosci* 2008; 27(7): 1801–8. <https://doi.org/10.1111/j.1460-9568.2008.06137.x>.
10. Gombkoto P, Rokszin A, Berenyi A, Braunitzer G, Utassy G, Benedek G, et al. Neuronal code of spatial visual information in the caudate nucleus. *Neuroscience* 2011; 182: 225–31. <https://doi.org/10.1016/j.neuroscience.2011.02.048>.
11. Rokszin A, Gombkoto P, Berenyi A, Markus Z, Braunitzer G, Benedek G, et al. Visual stimulation synchronizes or desynchronizes the activity of neuron pairs between the caudate nucleus and the posterior thalamus. *Brain Res* 2011; 1418: 52–63. <https://doi.org/10.1016/j.brainres.2011.08.015>.
12. Vicente AF, Bermudez MA, Romero Mdel C, Perez R, Gonzalez F. Putamen neurons process both sensory and motor information during a complex task. *Brain Res* 2012; 1466: 70–81. <https://doi.org/10.1016/j.brainres.2012.05.037>.
13. Nagypal T, Gombkoto P, Barkoczi B, Benedek G, Nagy A. Activity of caudate nucleus neurons in a visual fixation paradigm in behaving cats. *PLoS One* 2015; 10(11): e0142526. <https://doi.org/10.1371/journal.pone.0142526>.
14. Nagy A, Berenyi A, Wypych M, Waleszczyk WJ, Benedek G. Spectral receptive field properties of visually active neurons in the caudate nucleus. *Neurosci Lett* 2010; 480(2): 148–53. <https://doi.org/10.1016/j.neulet.2010.06.030>.
15. Hikosaka O, Takikawa Y, Kawagoe R. Role of the basal ganglia in the control of purposive saccadic eye movements. *Physiol Rev* 2000; 80(3): 953–78. <https://doi.org/10.1152/physrev.2000.80.3.953>.
16. Munoz DP, Fecteau JH. Vying for dominance: dynamic interactions control visual fixation and saccadic initiation in the superior colliculus. *Prog Brain Res* 2002; 140: 3–19. [https://doi.org/10.1016/S0079-6123\(02\)40039-8](https://doi.org/10.1016/S0079-6123(02)40039-8).



17. Nagypal T, Gombkoto P, Utassy G, Averkin RG, Benedek G, Nagy A. A new, behaving, head restrained, eye movement-controlled feline model for chronic visual electrophysiological recordings. *J Neurosci Methods* 2014; 221: 1–7. <https://doi.org/10.1016/j.jneumeth.2013.09.004>.
18. Franks NP, Zecharia AY. Sleep and general anesthesia. *Can J Anaesth* 2011; 58(2): 139–48. <https://doi.org/10.1007/s12630-010-9420-3>.
19. Kaisti KK, Langsjo JW, Aalto S, Oikonen V, Sipila H, Teras M, et al. Effects of sevoflurane, propofol, and adjunct nitrous oxide on regional cerebral blood flow, oxygen consumption, and blood volume in humans. *Anesthesiology* 2003; 99(3): 603–13. <https://doi.org/10.1097/00000542-200309000-00015>.
20. Barkoczi B, Nagypal T, Nyujto D, Katona X, Eordeghe G, Bodosi B, et al. Background activity and visual responsiveness of caudate nucleus neurons in halothane anesthetized and in awake, behaving cats. *Neuroscience* 2017; 356: 182–92. <https://doi.org/10.1016/j.neuroscience.2017.05.028>.
21. Villeneuve MY, Casanova C. On the use of isoflurane versus halothane in the study of visual response properties of single cells in the primary visual cortex. *J Neurosci Methods* 2003; 129(1): 19–31. [https://doi.org/10.1016/s0165-0270\(03\)00198-5](https://doi.org/10.1016/s0165-0270(03)00198-5).
22. Huxlin KR, Pasternak T. Training-induced recovery of visual motion perception after extrastriate cortical damage in the adult cat. *Cereb Cortex* 2004; 14(1): 81–90. <https://doi.org/10.1093/cercor/bhg106>.
23. Pigarev IN, Levichkina EV. Distance modulated neuronal activity in the cortical visual areas of cats. *Exp Brain Res* 2011; 214(1): 105–11. <https://doi.org/10.1007/s00221-011-2810-0>.
24. Pigarev IN, Rodionova EI. Two visual areas located in the middle suprasylvian gyrus (cytoarchitectonic field 7) of the cat's cortex. *Neuroscience* 1998; 85(3): 717–32. [https://doi.org/10.1016/s0306-4522\(97\)00642-8](https://doi.org/10.1016/s0306-4522(97)00642-8).
25. Populin LC, Yin TC. Behavioral studies of sound localization in the cat. *J Neurosci* 1998; 18(6): 2147–60. <https://doi.org/10.1523/JNEUROSCI.18-06-02147.1998>.
26. Populin LC, Yin TC. Bimodal interactions in the superior colliculus of the behaving cat. *J Neurosci* 2002; 22(7): 2826–34. <https://doi.org/10.1523/jneurosci.22-07-02826.2002>.
27. Tollin DJ, Populin LC, Moore JM, Ruhland JL, Yin TC. Sound-localization performance in the cat: the effect of restraining the head. *J Neurophysiol* 2005; 93(3): 1223–34. <https://doi.org/10.1152/jn.00747.2004>.
28. Korshunov VA. Miniature microdrive for extracellular recording of neuronal activity in freely moving animals. *J Neurosci Methods* 1995; 57(1): 77–80. [https://doi.org/10.1016/0165-0270\(94\)00130-9](https://doi.org/10.1016/0165-0270(94)00130-9).
29. McKown MD, Schadt JC. A modification of the Harper-McGinty microdrive for use in chronically prepared rabbits. *J Neurosci Methods* 2006; 153(2): 239–42. <https://doi.org/10.1016/j.jneumeth.2005.10.020>.
30. Brainard DH. The Psychophysics Toolbox. *Spat Vis* 1997; 10(4): 433–6.
31. Velly LJ, Rey MF, Bruder NJ, Gouwitsos FA, Witjas T, Regis JM, et al. Differential dynamic of action on cortical and subcortical structures of anesthetic agents during induction of anesthesia. *Anesthesiology* 2007; 107(2): 202–12. <https://doi.org/10.1097/01.anes.0000270734.99298.b4>.
32. Gevins A, Smith ME, McEvoy L, Yu D. High-resolution EEG mapping of cortical activation related to working memory: effects of task difficulty, type of processing, and practice. *Cereb Cortex* 1997; 7(4): 374–85. <https://doi.org/10.1093/cercor/7.4.374>.
33. Hsieh LT, Ekstrom AD, Ranganath C. Neural oscillations associated with item and temporal order maintenance in working memory. *J Neurosci* 2011; 31(30): 10803–10. <https://doi.org/10.1523/JNEUROSCI.0828-11.2011>.
34. Hsieh LT, Ranganath C. Frontal midline theta oscillations during working memory maintenance and episodic encoding and retrieval. *Neuroimage* 2014; 85(Pt 2): 721–9. <https://doi.org/10.1016/j.neuroimage.2013.08.003>.
35. Liebe S, Hoerzer GM, Logothetis NK, Rainer G. Theta coupling between V4 and prefrontal cortex predicts visual short-term memory performance. *Nat Neurosci* 2012; 15(3): 456–62. S1–2. <https://doi.org/10.1038/nn.3038>.



36. Roberts BM, Hsieh LT, Ranganath C. Oscillatory activity during maintenance of spatial and temporal information in working memory. *Neuropsychologia* 2013; 51(2): 349–57. <https://doi.org/10.1016/j.neuropsychologia.2012.10.009>.

37. Ergenoglu T, Demiralp T, Bayraktaroglu Z, Ergen M, Beydagl H, Uresin Y. Alpha rhythm of the EEG modulates visual detection performance in humans. *Brain Res Cogn Brain Res* 2004; 20(3): 376–83. <https://doi.org/10.1016/j.cogbrainres.2004.03.009>.

38. Schaefer RS, Vlek RJ, Desain P. Music perception and imagery in EEG: alpha band effects of task and stimulus. *Int J Psychophysiol* 2011; 82(3): 254–9. <https://doi.org/10.1016/j.ijpsycho.2011.09.007>.

39. Worden MS, Foxe JJ, Wang N, Simpson GV. Anticipatory biasing of visuospatial attention indexed by retinotopically specific alpha-band electroencephalography increases over occipital cortex. *J Neurosci* 2000; 20(6): RC63. <https://doi.org/10.1523/jneurosci.20-06-j0002.2000>.

40. Foxe JJ, Snyder AC. The role of alpha-band brain oscillations as a sensory suppression mechanism during selective attention. *Front Psychol* 2011; 2: 154. <https://doi.org/10.3389/fpsyg.2011.00154>.

41. Michels L, Moazami-Goudarzi M, Jeanmonod D, Sarnthein J. EEG alpha distinguishes between cuneal and precuneal activation in working memory. *Neuroimage* 2008; 40(3): 1296–310. <https://doi.org/10.1016/j.neuroimage.2007.12.048>.

42. Puszta A, Pertich A, Katona X, Bodosi B, Nyujto D, Giricz Z, et al. Power-spectra and cross-frequency coupling changes in visual and Audio-visual acquired equivalence learning. *Sci Rep* 2019; 9(1): 9444. <https://doi.org/10.1038/s41598-019-45978-3>.

43. Gombkoto P, Berenyi A, Nagypal T, Benedek G, Braunitzer G, Nagy A. Co-oscillation and synchronization between the posterior thalamus and the caudate nucleus during visual stimulation. *Neuroscience* 2013; 242: 21–7. <https://doi.org/10.1016/j.neuroscience.2013.03.028>.

44. Blake R, Sloane M, Fox R. Further developments in binocular summation. *Percept Psychophys* 1981; 30(3): 266–76. <https://doi.org/10.3758/bf03214282>.

45. di Summa A, Polo A, Tinazzi M, Zanette G, Bertolasi L, Bongiovanni LG, et al. Binocular interaction in normal vision studied by pattern-reversal visual evoked potential (PR-VEPS). *Ital J Neurol Sci* 1997; 18(2): 81–6. <https://doi.org/10.1007/BF01999567>.

46. Mitchell BA, Dougherty K, Westerberg JA, Carlson BM, Daumail L, Maier A, et al. Stimulating both eyes with matching stimuli enhances V1 responses. *iScience* 2022; 25(5): 104182. <https://doi.org/10.1016/j.isci.2022.104182>.

47. Herreras O. Local field potentials: myths and misunderstandings. *Front Neural Circuits* 2016; 10: 101. <https://doi.org/10.3389/fncir.2016.00101>.

---

**Open Access statement.** This is an open-access article distributed under the terms of the Creative Commons Attribution 4.0 International License (<https://creativecommons.org/licenses/by/4.0/>), which permits unrestricted use, distribution, and reproduction in any medium, provided the original author and source are credited, a link to the CC License is provided, and changes – if any – are indicated. (SID\_1)

